Structure determination of a planar defect in $SrBi_2Ta_2O_9$

Y. Yan[a] and M. M. Al-Jassim
National Renewable Energy Laboratory, Golden, Colorado 80401

Z. Xu, X. Lu, D. Viehland, and M. Payne
Department of Materials Science and Engineering, University of Illinois, Urbana, Illinois 61801

S. J. Pennycook
Solid State Division, Oak Ridge National Laboratory, Oak Ridge, Tennessee 37831

(Received 2 June 1999; accepted for publication 29 July 1999)

The atomic structure of a planar defect with a (001) habit plane in single crystal layered perovskite $SrBi_2Ta_2O_9$ is determined by high-resolution *Z*-contrast imaging. We found that the defect forms a structure, with two Sr–Ta–O perovskite blocks connected by a metallic Sr_2 plane, rather than a Bi_2O_2 layer as in the perfect crystal. This defect is expected to be an efficient hole trap and may have important implications for the electronic properties and the ferroelectric response of the $SrBi_2Ta_2O_9$ material. © *1999 American Institute of Physics.* [S0003-6951(99)03039-9]

Ferroelectric materials have received much attention because of their nonvolatile ferroelectric random access memory (NvFRAM) applications.[1–3] Recently, $SrBi_2Ta_2O_9$, a bismuth-layered ferroelectric compound, has been recognized as a leading candidate for NvFRAM applications because of its negligible fatigue, low leakage currents, and ability to maintain bulk characteristics when fabricated in very thin films.[4–6] It has been suggested that fatigue in ferroelectric materials such as $Pb(Zr,Ti)O_3$ is a result of relatively high pinning energies for domain walls.[7,8] The absence of fatigue in $SrBi_2Ta_2O_9$ is thought to be due to the fact that electronic traps in this material are shallow, which results in weak pinning of domain walls so that they are more easily depinned by an external field.[8,9] Thus, factors that can influence electronic trap states in $SrBi_2Ta_2O_9$, e.g., impurities and defects, are critically important to the properties of this material. While most work to date has focused on thin film forms for nonvolatile memory applications,[10–13] its basic structure, intrinsic properties, and the effects of defects on these properties are not well understood, mainly because of the lack of large single crystals and well-characterized defects. In this letter, we report a direct determination of a planar defect structure in $SrBi_2Ta_2O_9$, using high-resolution *Z*-contrast imaging.

$SrBi_2Ta_2O_9$ single crystals were grown by a flux solution method using excess Bi_2O_3 as a self flux. Specimens were prepared for electron microscopy by first cutting the bulk material into (110) slices, followed by mechanical polishing to ~100 μm, then dimpling the central portion of the specimens to ~10 μm. Samples were thinned to electron transparency using a 4 kV Ar ion beam at a 13° inclination and then cleaned at lower voltage (1.5 kV). Finally, surface contamination was removed using a Fischione plasma cleaner. High-resolution imaging was performed using a VG Microscopes HB603U STEM operating at 300 kV. *Z*-contrast images were formed by scanning a 1.26 Å probe across a specimen and recording the transmitted high-angle scattering with an annular detector. The *Z*-contrast image is incoherent, with intensity highly localized about the atomic column positions.[14,15] The image intensity is approximately proportional to the mean square atomic number (Z) in the columns.

$SrBi_2Ta_2O_9$ is one of a family of Bi-containing layered-perovskite materials. Its structure has been refined by x-ray and electron diffraction ($a=5.53$ Å, $b=5.53$ Å, $c=24.98$ Å),[16] and contains Sr–Ta–O perovskite blocks created by Ta–O octahedra inside which a 12-fold cation (Sr) resides. These perovskite blocks are connected by Bi_2O_2 layers. Figure 1 shows the projected structure of $SrBi_2Ta_2O_9$ along the [110] axis. The large open circles indicate Bi, hatched circles indicate Ta, solid circles indicate Sr, and small open circles indicate O. The diamond shapes indicated by solid lines represent Ta–O octahedra. The Sr–Ta–O blocks and Bi_2O_2 layers are indicated in Fig. 1

Figure 2(a) shows a low magnification *Z*-contrast image of $SrBi_2Ta_2O_9$ taken along the [110] zone axis, but with the layered structure resolved. It clearly shows the stacking of alternate Bi_2O_2 layers and Sr–Ta–O perovskite blocks, as indicated by the letters B and P, respectively. The Ta and Bi columns have high intensities, the Sr columns lower intensities, while the pure O columns are not seen because of the low atomic number ($Z=8$) of oxygen. The Bi ($Z=83$) and

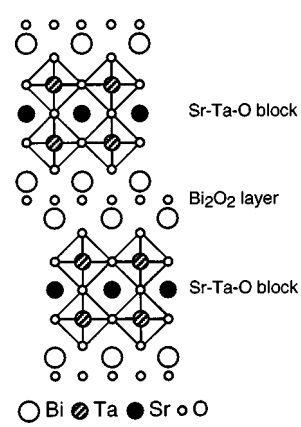

FIG. 1. Projection of the structure of $SrBi_2Ta_2O_9$ along the [110] axis.

[a]Electronic mail: yyan@nrel.gov

 © 1999 American Institute of Physics
Downloaded 04 Jun 2004 to 160.91.48.238. Redistribution subject to AIP license or copyright, see http://apl.aip.org/apl/copyright.jsp

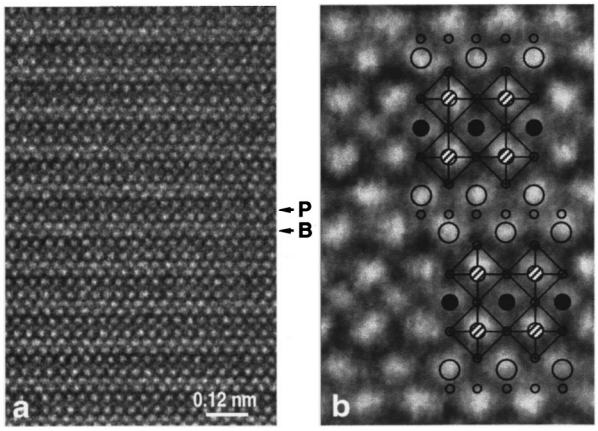

FIG. 2. (a) Low magnification *Z*-contrast image of $SrBi_2Ta_2O_9$ taken along the [110] zone axis; (b) high-resolution *Z*-contrast image showing the atomic structure.

Ta ($Z=73$) columns have very little difference in intensity because of the relatively small difference of atomic number between them. The sensitivity is limited by surface damage formed during ion milling, which can cause intensity fluctuations on the order of $\pm 10\%$. The Sr columns show low intensity (see the middle line in the block indicated by P) because of the lower atomic number ($Z=38$). A high magnification *Z*-contrast image is given in Fig. 2(b). Superimposing the structure shown in Fig. 1 on the image gives an excellent fit, demonstrating that the single crystal sample observed is of high quality despite the complex $SrBi_2Ta_2O_9$ structure, which has a repeat distance along [001] of 24.98 Å.

Figure 3(a) shows a low magnification *Z*-contrast image

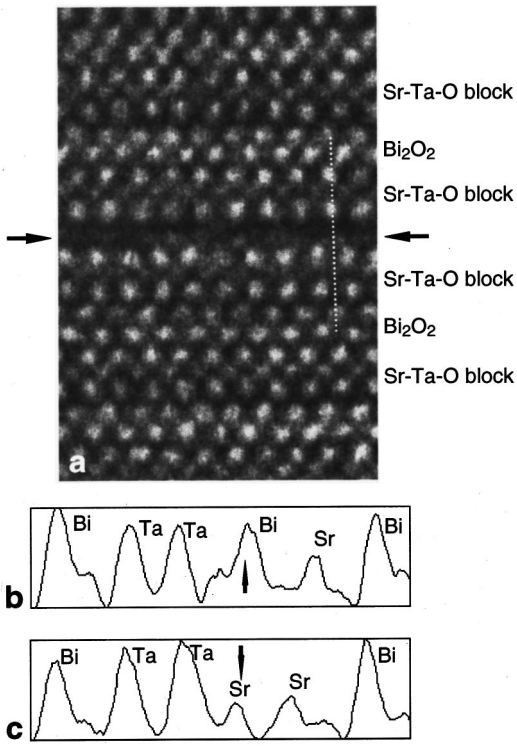

FIG. 3. (a) *Z*-contrast image of $SrBi_2Ta_2O_9$ taken from an area containing a planar defect lying on the (001) plane; (b) intensity profile measured from a perfect area; (c) intensity profile measured from the area containing the defect.

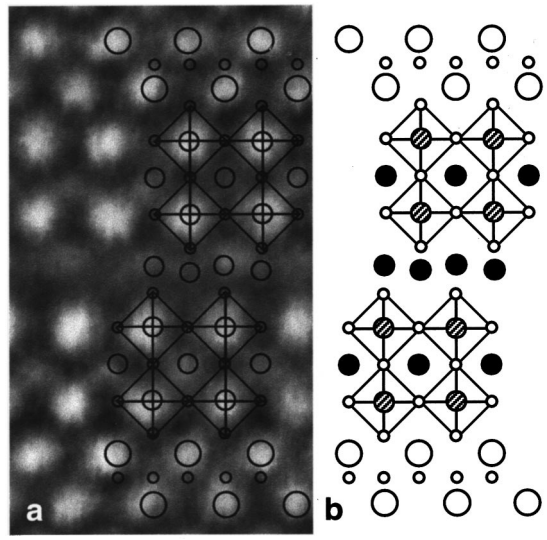

FIG. 4. (a) High-resolution *Z*-contrast image of the planar defect; (b) the atomic structure of the defect derived directly from the image.

of $SrBi_2Ta_2O_9$ taken from an area containing a planar defect. The electron beam is parallel to the [110] axis. As indicated by the two arrows, a defect lying on the (001) plane is clearly seen. The Sr–Ta–O perovskite blocks and Bi_2O_2 layers in the bulk near the defect are indicated. It is seen that two Sr–Ta–O perovskite blocks at the defect are connected by a layer with significantly lower intensity than that of perfect Bi_2O_2 layers. The intensity profiles measured along the direction indicated by the white dotted line in Fig. 3(a) from both a perfect region and the region containing the defect are shown in Figs. 3(b) and 3(c), respectively. The position of the defect in Fig. 3 is indicated by arrows. The intensity strongly suggests that the columns at the defect plane are Sr columns.

Figure 4(a) shows a high magnification *Z*-contrast image of the defect from which the atomic structure can be obtained directly, as shown in Fig. 4(b). The large open circles indicate Bi, hatched circles indicate Ta, solid circles indicate Sr, and small open circles indicate O. The diamond shapes indicated by solid lines represent Ta–O octahedra. Superimposing this structure on the image provides a very good fit, as shown. This planar defect presents a structure in that two neighboring Sr–Ta–O perovskite blocks are connected not by a Bi_2O_2 layer, as in the perfect crystal, but by a Sr–O plane. This Sr–O plane shows double the expected number of Sr columns, compared to the Sr–O plane in the Sr–Ta–O perovskite blocks. Also, the distance between the two Sr–Ta–O perovskite blocks at the defect is about 1.2 Å smaller than in the perfect region. The differences between the defect and the perfect crystal are clearly seen by comparing the structure of the defects shown in Fig. 4(a) and the perfect crystal shown in Fig. 2(b). It seems unlikely that the defect plane can contain oxygen, otherwise we would anticipate that a double layer of SrO planes would take the rocksalt structure, the supper and lower planes, matching the upper and lower perovskite blocks, with a half unit-cell displacement between them. The observed 1.2 Å inward relaxation of the structure also suggests that the plane is metallic. The Sr atom position relative to each Ta–O octahedron is identical to that of the Bi atoms in the Bi_2O_2 layer, and thus, the defect

Downloaded 04 Jun 2004 to 160.91.48.238. Redistribution subject to AIP license or copyright, see http://apl.aip.org/apl/copyright.jsp

looks like a Bi_2O_2 layer with the central O layer removed. We note, however, that the precise composition of the Sr_2 layer cannot be obtained from the intensity profile measured from the *Z*-contrast images due to the varying intensities of columns along the layer. Such effects could indicate local strains and/or the possible existence of vacancies in this layer. The absence of the central oxygen plane in the defect is consistent with the lower oxidation state of Sr^{2+} compared to Bi^{3+}. For a neutral unit cell, the Sr would be in a Sr^0 state, suggesting that the defect would act as an efficient hole trap.

Theoretical calculations have suggested that the displacements of Ta ions along O–Ta–O bonds in the *ab* plane are largely responsible for the ferroelectricity of $SrBi_2Ta_2O_9$.[9] It has been suggested that the Bi–O layers dominate the electronic response of $SrBi_2Ta_2O_9$, whereas the ferroelectric response originates from the Sr–Ta–O perovskite blocks. However, Bi displacements amplify the ferroelectric dipole. The contribution could be large because the Bi displacements can be substantial, due to the weaker bonding of the Bi–O layer. The absence of a Bi–O layer at the defect will therefore weaken this contribution to the ferroelectricity and affect the ferroelectric response, although the overall effect should be small because of the low volume fraction within the bulk. The effect on carrier trapping is likely to be more important. It is suggested that fatigue is fundamentally related to the trapping of electronic carriers, which then pin domain walls. In $SrBi_2Ta_2O_9$, the weak pinning of domain walls is considered to be the reason for its good fatigue resistance. Proposed candidates for the trap states are holes trapped at Bi^{3+} ions or electrons trapped at Ta^{5+}.[9] The appearance of planar defects with metallic Sr_2 layers would clearly act as strong hole trapping centers and increase the overall pinning effect. Thus, we propose that this defect may also have considerable effect on fatigue resistance of $SrBi_2Ta_2O_9$.

In conclusion, we have determined the atomic structure of a planar defect in single crystal $SrBi_2Ta_2O_9$ by high-resolution *Z*-contrast imaging. The defect consists of two Sr–Ta–O perovskite blocks connected by a metallic Sr_2 plane. The defect is expected to be a strong hole trap, which may have considerable effects on the ferroelectric properties of this material.

The authors would like to express their thanks to A. Kadavanich for helpful discussions. The work at NREL was supported by the U.S. Department of Energy under Contract No. DE-AC36-98GO10337; at ORNL, this work was sponsored by the Division of Materials Sciences, U.S. Department of Energy, under Contract No. DE-AC05-96OR22464 with Lockheed Martin Energy Research Corporation. The research at UIUC was sponsored by the Basic Energy Sciences, U.S. Department of Energy, under Contract No. DEF602-96ER45439.

[1] J. F. Scott and C. A. Paz de Araujo, Science **246**, 1400 (1989).
[2] S. Dey and R. Zuleeg, Ferroelectrics **108**, 37 (1990).
[3] G. H. Haerting, J. Vac. Sci. Technol. A **9**, 414 (1990).
[4] C. A. Paz de Araujo, J. D. Cuchiaro, L. D. McMillan, M. C. Scott, and J. F. Scott, Nature (London) **374**, 627 (1995).
[5] S. B. Desu and D. P. Vijay, Mater. Sci. Eng., B **32**, 83 (1995).
[6] J. F. Scott, F. M. Ross, C. A. Paz de Araujo, M. C. Scott, and M. Huffman, MRS Bull. **21**, 33 (1996).
[7] H. N. Al-Shareef, D. Dimos, T. J. Boyle, W. L. Warren, and B. A. Tuttle, Appl. Phys. Lett. **68**, 690 (1996).
[8] D. Dimos, H. N. Al-Shareef, W. L. Warren, and B. A. Tuttle, J. Appl. Phys. **80**, 1682 (1996).
[9] J. Robertson, C. W. Chen, W. L. Warren, and C. D. Gutleben, Appl. Phys. Lett. **69**, 1704 (1996).
[10] K. Amanuna, T. Hase, and Y. Miyasaka, Appl. Phys. Lett. **66**, 221 (1995).
[11] P. C. Joshi, S. O. Ryu, X. Zhang, and S. B. Desu, Appl. Phys. Lett. **70**, 1080 (1997).
[12] K. Watanabe, A. J. Hartmann, R. N. Lamb, and J. F. Scott, J. Appl. Phys. **84**, 2170 (1998).
[13] Z. G. Zhang, J. S. Liu, Y. N. Wang, J. S. Zhu, D. Su, and H. M. Shen, Appl. Phys. Lett. **85**, 1746 (1999).
[14] S. J. Pennycook and D. E. Jesson, Phys. Rev. Lett. **64**, 938 (1990).
[15] S. J. Pennycook and D. E. Jesson, Ultramicroscopy **37**, 14 (1991).
[16] A. D. Rae, J. G. Thompson, and R. L. Withers, Acta Crystallogr., Sect. B: Struct. Sci. **48**, 418 (1992).

Downloaded 04 Jun 2004 to 160.91.48.238. Redistribution subject to AIP license or copyright, see http://apl.aip.org/apl/copyright.jsp